Published in final edited form as:
Nat Genet. 2012 May ; 44(5): 581–585. doi:10.1038/ng.2253.

Mutations in *ISPD* cause Walker-Warburg syndrome and defective glycosylation of α-dystroglycan

Tony Roscioli[1,2,20], **Erik-Jan Kamsteeg**[1,20], **Karen Buysse**[1,20], **Isabelle Maystadt**[3,20], **Jeroen van Reeuwijk**[1], **Christa van den Elzen**[1], **Ellen van Beusekom**[1], **Moniek Riemersma**[1,4], **Rolph Pfundt**[1], **Lisenka E.L.M. Vissers**[1], **Margit Schraders**[5], **Umut Altunoglu**[6], **Michael F. Buckley**[1,2], **Han G. Brunner**[1], **Bernard Grisart**[3], **Huiqing Zhou**[1], **Joris A. Veltman**[1], **Christian Gilissen**[1], **Grazia M.S. Mancini**[7], **Paul Delrée**[3], **Michèl A. Willemsen**[4], **Danijela Petković Ramadža**[8], **David Chitayat**[9,10], **Christopher Bennett**[11], **Eamonn Sheridan**[11], **Els A.J. Peeters**[12], **Gita M.B. Tan-Sindhunata**[13], **Christine E. de Die-Smulders**[14], **Koenraad Devriendt**[15], **Hülya Kayserili**[6], **Osama Abd El-Fattah El-Hashash**[16,17], **Derek L. Stemple**[18], **Dirk J. Lefeber**[4,19], **Yung-Yao Lin**[18,21], and **Hans van Bokhoven**[1,21]

[1]Department of Human Genetics, Nijmegen Centre for Molecular Life Sciences, Radboud University Nijmegen Medical Centre, Nijmegen, The Netherlands [2]School of Women's and Children's Health, Sydney Children's hospital and the University of New South Wales, Sydney, Australia [3]Centre de Génétique Humaine, Institut de Pathologie et de Génétique, Gosselies, Belgium [4]Department of Neurology, Radboud University Nijmegen Medical Centre, Nijmegen, The Netherlands [5]Department of Otorhinolaryngology, Nijmegen Centre for Molecular Life Sciences, Radboud University Nijmegen Medical Centre, Nijmegen [6]Medical Genetics Department, Istanbul Medical Faculty, Istanbul University, Istanbul, Turkey [7]Department of Clinical Genetics, Erasmus MC, Rotterdam, The Netherlands [8]Department of Pediatrics, University Hospital Centre, Zagreb, Croatia [9]Mount Sinai Hospital, The Prenatal Diagnosis and Medical Genetics Program, Department of Obstetrics and Gynecology, University of Toronto, Toronto, Canada [10]The Hospital for Sick Children, Division of Clinical and Metabolic Genetics, Toronto, Canada [11]Department of Clinical Genetics, St James's University Hospital, Leeds, United Kingdom [12]Medisch Centrum Haaglanden, Den Haag, The Netherlands [13]Department of Clinical Genetics, VU University Medical Center, Amsterdam, The Netherlands [14]Department of Clinical Genetics, Maastricht University Medical Centre, Maastricht, The Netherlands [15]Center for Human Genetics, Clinical Genetics, Catholic University Leuven, Leuven, Belgium [16]Pediatric department, Farwaniya Hospital, Kuwait City, Kuwait [17]Ministry of Health, Cairo, Egypt

Correspondence: Yung-Yao Lin, PhD, Wellcome Trust Sanger Institute, Wellcome Trust Genome Campus, Hinxton, Cambridge, CB10 1SA, United Kingdom, and Hans van Bokhoven, PhD, Department of Human Genetics 855, Radboud University Nijmegen Medical Centre, Nijmegen, P.O. Box 9101, 6500 HB Nijmegen, The Netherlands. YYL@sanger.ac.uk & H.vanbokhoven@gen.umcn.nl.
[20]These authors contributed equally to this work
[21]These authors jointly directed this work.

URLs UCSC Genome Bioinformatics, http://www.genome.ucsc.edu/; OMIM and Unigene, http://www.ncbi.nlm.nih.gov/; Ensembl, http://www.ensembl.org/index.html; PolyPhen2 http://genetics.bwh.harvard.edu/pph2/; Project HOPE http://www.cmbi.ru.nl/hope/home; Exome Variant Server http://snp.gs.washington.edu/EVS/; ZFIN http://www.zfin.org/

AUTHOR CONTRIBUTIONS The study was designed and the results were interpreted by T.R., K.B., D.L.S., Y.Y.L., H.G.B., D.J.L. and H.V.B. Subject ascertainment and recruitment was carried out by I.M., U.A., B.G., G.M.S.M., P.D., M.A.W., D.P.R., D.C., C.B., E.S., E.A.J.P., G.M.B.T.S., C.E.D.D.S., K.D., H.K., O.A.E.F.E.H., and H.V.B. Sequencing, CNV analysis and genotyping was carried out and interpreted by T.R., E.J.K., K.B., I.M., J.V.R., C.V.D.E., E.V.B., M.R., R.P., L.E.L.M.V., M.S., M.F.B., H.Z., J.A.V., C.G., G.M.S.M., and H.V.B. Zebrafish studies were designed and carried out by K.B., D.L.S. and Y.Y.L. Bioinformatic data analysis and protein modeling was done by T.R., J.V.R., C.G., and D.J.L. The manuscript was drafted by T.R., K.B., D.J.L., Y.Y.L. and H.V.B. All authors contributed to the final version of the paper.

COMPETING FINANCIAL INTERESTS The authors declare that they have no competing financial interests.

Europe PMC Funders Author Manuscripts

[18]Wellcome Trust Sanger Institute, Wellcome Trust Genome Campus, Hinxton, Cambridge, CB10 1SA, United Kingdom [19]Laboratory for Genetic, Endocrine and Metabolic Disease, Radboud University Nijmegen Medical Centre, Nijmegen, The Netherlands

Abstract

Walker-Warburg syndrome (WWS) is an autosomal recessive multisystem disorder characterized by complex eye and brain abnormalities with congenital muscular dystrophy (CMD) and aberrant α-dystroglycan (αDG) glycosylation. Here, we report mutations in the *isoprenoid synthase domain-containing (ISPD*) gene as the second most common cause of WWS. Bacterial IspD is a nucleotidyl transferase belonging to a large glycosyltransferase family, but its role in chordates has been obscure to date because this phylum does not have the corresponding non-mevalonate isoprenoid biosynthesis pathway. Knockdown of *ispd* in zebrafish recapitulates the human WWS phenotype with hydrocephalus, reduced eye size, muscle degeneration and hypoglycosylated αDG. These results implicate a role for ISPD in αDG glycosylation to maintain sarcolemma integrity in vertebrates.

Defective O-linked glycosylation of αDG is the characteristic feature of a clinically and genetically heterogeneous group of disorders, commonly referred to as dystroglycanopathies. This group of diseases is characterized by a broad phenotypic spectrum ranging from severe forms of CMD with eye involvement, cerebral malformations and intellectual disability including WWS and Muscle Eye Brain disease (MEB), to milder adult-onset phenotypes without central nervous system involvement such as limb girdle muscular dystrophy (LGMD) type 2I[1]. Mutations in six genes, *POMT1*, *POMT2*, *POMGnT1*, *FKTN*, *FKRP* and *LARGE*, encoding proteins involved in the post-translational modification of αDG, have been implicated in WWS and other dystroglycanopathies[1-10]. Mutations in these six genes represent 35% of WWS incidence, suggesting that additional WWS genes await discovery. At the milder end of the dystroglycanopathy disease spectrum single patients have been reported with αDG hypoglycosylation due to a missense mutation in either the dystroglycan gene (*DAG1*)[11] or the *DPM3* gene[12], the latter leading to reduced levels of dolichol-P-mannose donor for O-mannosylation[12]. The factors determining dystroglycanopathy phenotypes are not well understood, but may involve the extent of residual glycosylation of αDG[1,13,14] and other proteins[15-17]. Identifying novel causative genes will shed light on the pathological mechanisms of WWS and other dystroglycanopathies.

To identify novel genes that are involved in WWS, we selected a cohort of 59 patients with idiopathic WWS in whom mutations in the known dystroglycanopathy genes had been previously excluded. Thirty of these patients, the majority of whom came from consanguineous families, were genotyped using the Affymetrix GeneChip Human Mapping 250K SNP *Nsp*I Array to identify copy number variants (CNVs) and homozygous regions. SNP haplotyping detected a large number of non-overlapping homozygous regions amongst these patients, providing support for further genetic heterogeneity in WWS (Supplementary Fig. 1). Interestingly, the corresponding CNV profiles identified two homozygous deletions affecting the *ISPD* gene (patients WWS-160 and WWS-161, Supplementary Fig. 2), suggesting that *ISPD* is a strong candidate for WWS, as there were no other overlapping CNV regions present in the patient cohort. Another family (WWS-25; for pedigree see Supplementary Fig. 3a) was identified with two siblings and a cousin affected with WWS who shared a 3.5 Mb homozygous region on chromosome 7p21 containing ten genes including *ISPD* (Fig. 1a). One of these siblings was investigated by exome sequencing and after filtering based on an autosomal recessive pattern of inheritance according to methods

described previously[18], a single homozygous variant was identified in this region of shared homozygosity. This c.647C>A transversion in exon 3 of *ISPD* (NM_001101426.3), predicting a p.Ala216Asp substitution, showed complete segregation in the family, being present in the homozygous state in the other two affected individuals, in the heterozygous state in both parental couples and absent in healthy or deceased siblings with another phenotype.

Next, we sequenced the ten coding exons of *ISPD* in the WWS patient cohort and identified missense, nonsense and frameshift mutations in an additional five individuals from five families (Supplementary Fig. 3). In addition, failure to PCR-amplify exons 3 to 5 in family WWS-37, suggested the presence of a homozygous intragenic microdeletion, which was confirmed by quantitative MLPA analysis (data not shown). An overview of all identified mutations is given in Table 1 and a schematic representation of their localization is shown in Figure 1a. In summary, mutations affecting *ISPD* were detected in 9 out of 94 families, accounting for an overall percentage of 10% (Fig. 1b). All mutations showed a segregation pattern expected for causative recessive mutations in family members available for testing and were absent in a control cohort of 3712 haploid genomes. The three nonsense mutations, p.Arg268*, p.Lys278* and p.Glu396*, are predicted to give rise to nonsense-mediated mRNA decay or truncation of the protein. The three missense mutations (p.Ala216Asp, p.Arg126His and p.Ala122Pro) are located within the ISPD domain (Fig. 1a; Supplementary Fig. 4a), a conserved domain of a large GT-A glycosyltransferase family that also includes nucleotidyltransferases[19]. Both p.Ala216Asp and p.Arg126His affect highly conserved amino acids and are predicted to be damaging by PolyPhen2, whereas p.Ala122Pro is predicted to be probably damaging. *In silico* modeling based on an *E. coli* IspD crystal structure using the HOPE web server (see URLs) predicted charge and size differences between the wild-type and mutant amino acids that are likely to affect protein folding and disruption of the CTP-binding pocket for mutations p.Ala122Pro and p.Arg126His (Supplementary Fig. 4b).

All affected individuals with *ISPD* mutations had a severe WWS-like phenotype with only two out of 11 surviving beyond two years of age with brain anomalies that are more indicative of MEB (WWS-81 and -163; Supplementary Table 1). Routine cerebral MRI (Fig. 2a and 2b) showed typical features of cobblestone lissencephaly together with hydrocephalus, cerebellar hypoplasia and a kinked brainstem. Muscle histology and immunohistochemistry showed dystrophic changes and clear reduction of glycosylated αDG by the IIH6 antibody, which recognizes an unknown glyco-epitope on αDG[20] (patients from families WWS-25, -160, and -81) (Fig. 2c-f).

The function of ISPD in vertebrates is unknown. In view of the significant conservation of protein sequences (65% amino acid similarity) between the zebrafish (*Danio rerio*) and human orthologs, we determined the effects of loss of function of zebrafish *ispd*, which encodes two isoforms that differ only in their N-termini. To do this, we knocked down both *ispd* isoforms with antisense morpholino oligonucleotides (MO), targeting exon-intron splice sites common to both transcripts (Supplementary Fig. 5). High doses of *ispd* MO1 (7 ng) caused hydrocephalus and incomplete brain folding in 82% of embryos (n=88) by 48 hours post fertilization (h.p.f.) (Fig. 3a and Supplementary Fig. 6), as well as significantly reduced eye size reminiscent of microphthalmia in WWS patients (Fig. 3b and 3c). Other phenotypic features included impaired motility and myotome lesions (data not shown). Injection of *ispd* MO2 (3 ng) caused similar morphological abnormalities, assuring the specificity of both MOs (Supplementary Fig. 7). We looked for structural defects in muscle fibers by labeling sarcolemma with membrane-localized red fluorescent protein (mRFP) and filamentous-actin (F-actin) with phalloidin. *ispd* MO1-injected embryos showed muscle fiber degeneration by 72 h.p.f. (Fig. 3d) and, in some cases, disruption of myotendinous

junctions (MTJ; 45%, n=31), exemplified by elongated muscle fibers spanning MTJ (Fig. 3d). Together, these results suggest that zebrafish *ispd* knockdown embryos recapitulate the major aspects of human WWS pathology.

Hypoglycosylation of αDG is a diagnostic characteristic of WWS. To test if knockdown of *ispd* in zebrafish also affects glycosylation of αDG, we performed western blotting with the IIH6 antibody[20]. Compared with control embryos, glycosylated αDG was reduced in *ispd* MO1-injected zebrafish embryos (Fig. 4a). Given the similarity of MTJ disruption observed in *ispd* MO1-injected embryos and zebrafish laminin mutants[21,22], the localization of laminins was assessed. Despite the severe muscle fiber degeneration, laminins remained localized to the MTJ in *ispd* MO1-injected embryos (Fig. 4b). Subsequently, we assessed the sarcolemma integrity in embryos injected with either *ispd* MO using Evans blue dye (EBD). Intact sarcolemma is impermeable to EBD. We found that MTJ-anchored muscle fibers were infiltrated by EBD before the onset of muscle degeneration at 48 h.p.f. (Fig. 4c and Supplementary Fig. 7c). Muscle pathology became evident as EBD-infiltrated muscle fibers retracted during muscle degeneration. The posterior myotome of *ispd* MO1-injected embryos was more susceptible to sarcolemma damage than the anterior myotome (Fig. 4c). As sarcolemma damage was reported in dystrophin-deficient models[23,24], we assessed the immunoreactivity of dystrophin in *ispd* MO1-injected embryos. No obvious alterations to dystrophin immunoreactivity were detected (data not shown). Together, these results demonstrate an important WWS pathogenic mechanism, independent from laminin and dystrophin, in which loss of Ispd function in zebrafish results in αDG hypoglycosylation and compromised sarcolemma integrity, preceding muscle fiber degeneration.

In plants, protozoa and some bacteria, ISPD belongs to the non-mevalonate isoprenoid biosynthesis (MEP) pathway, which is absent in vertebrates[25]. Prokaryotic IspD has cytidyltransferase activity using 2-C-methyl-D erythritol as substrate for the synthesis of the nucleotide sugar CDP-methyl-erythritol. The structurally homologous TarI in *Streptococcus pneumoniae*, lacking the MEP pathway, uses ribitol-1-phosphate to produce an activated nucleotide sugar (CDP-ribitol) used for incorporation in polysaccharides[26]. Analogous to the role of DPM3, it is likely that human ISPD synthesises a novel nucleotide sugar, the exact nature of which remains to be determined. Glycosyltransferases could use such nucleotide-activated building blocks for incorporation into the αDG O-mannosyl glycan. Intriguingly, the bacterium *Prevotella tannerae* expresses a gene (accession number ZP_05736246) with both IspD and LicD (*li*popolysaccharide *c*ore *D*) domains, which may act sequentially in the post-translational modifications. The LicD domain is also found in the putative glycosyltransferases, FKTN and FKRP, both involved in the glycosylation of αDG. Thus, it appears that the ISPD and LicD domains that are both contained in a prokaryotic precursor protein are dispersed over the vertebrate ISPD and FKTN/FKRP proteins, respectively. We sought to test the possibility of genetic interactions between these genes. Co-injection of sub-effective doses of *ispd* MO1 with *fktn* or *fkrp* MO showed a marked increase in the proportion of embryos with hydrocephalus (68% and 49% respectively, compared with 3% in control MO and *ispd* MO1 co-injection; Fig. 4d and Supplementary Fig. 8a). The same effect was seen using *ispd* MO2, confirming specificity (Supplementary Fig. 8). Moreover, glycosylation of αDG is reduced in the embryos co-injected with *ispd* MO1 and *fktn/fkrp* MO as compared to embryos co-injected with *ispd* MO1 and control MO, and single *fktn/fkrp* MO-injected embryos (Fig. 4e). These results support a cooperative interaction between *ispd* and *fktn/fkrp* in αDG glycosylation.

In conclusion, our findings provide evidence for a significant contribution of *ISPD* mutations to the prevalence of WWS. We report the identification of *ISPD* mutations in nine WWS families. Due to the high frequency of *ISPD* mutations in this WWS cohort (15% of pre-screened patients, 10% overall, Fig. 1b), we recommend that *ISPD* mutation analysis

should be performed as part of routine molecular diagnostic testing in WWS. With the identification of ISPD, we can now explain almost 50% of all WWS of our cohort. The results of homozygosity mapping indicate the existence of several additional loci. Given that most of the remaining patients represent isolated cases, we anticipate that exome sequencing will be the strategy of choice to resolve additional genes and to unravel the complex post-translational modification pathways that are key to normal brain and muscular development.

Supplementary Material

Refer to Web version on PubMed Central for supplementary material.

Acknowledgments

We thank all family members who participated in this study. We would also like to thank A. Charon, Service de Pédiatrie, Grand Hôpital de Charleroi, Charleroi, Belgium for referring an affected patient, G. Powell and S. Gerety for critical comments on the manuscript and R. Schot for study of the deletion in family WWS-161. This project was supported by the Large-Scale Integrating Project GENCODYS-Genetic and Epigenetic Networks in Cognitive DYSfunction (241995), which is funded by the EU FP7 Health program (HvB), the Australian NHMRC with an overseas post-doctoral fellowship (TR), The Prinses Beatrix Fund (grant W.OR09-15 to DL and HvB), the Hersenstichting Nederland (HvB), and an EMBO Long-Term Fellowship (ALTF 805-2009 to KB). All zebrafish work was sponsored by the Wellcome Trust [grant number WT 077047/Z/05/Z] and [grant number WT 077037/Z/05/Z]. NGS experiments were financially supported by the Department of Human Genetics, Nijmegen, The Netherlands, as well as by the Netherlands Organization for Health Research and Development (ZonMW grant 916-86-016 to LELMV).

REFERENCES

1. van Reeuwijk J, Brunner HG, van Bokhoven H. Glyc-O-genetics of Walker-Warburg syndrome. Clin Genet. 2005; 67:281–9. [PubMed: 15733261]
2. Kobayashi K, et al. An ancient retrotransposal insertion causes Fukuyama-type congenital muscular dystrophy. Nature. 1998; 394:388–92. [PubMed: 9690476]
3. Yoshida A, et al. Muscular dystrophy and neuronal migration disorder caused by mutations in a glycosyltransferase, POMGnT1. Dev Cell. 2001; 1:717–24. [PubMed: 11709191]
4. Beltran-Valero de Bernabe D, et al. Mutations in the O-mannosyltransferase gene POMT1 give rise to the severe neuronal migration disorder Walker-Warburg syndrome. Am J Hum Genet. 2002; 71:1033–43. [PubMed: 12369018]
5. Brockington M, et al. Mutations in the fukutin-related protein gene (FKRP) cause a form of congenital muscular dystrophy with secondary laminin alpha2 deficiency and abnormal glycosylation of alpha-dystroglycan. Am J Hum Genet. 2001; 69:1198–209. [PubMed: 11592034]
6. Longman C, et al. Mutations in the human LARGE gene cause MDC1D, a novel form of congenital muscular dystrophy with severe mental retardation and abnormal glycosylation of alpha-dystroglycan. Hum Mol Genet. 2003; 12:2853–61. [PubMed: 12966029]
7. Beltran-Valero de Bernabe D, et al. Mutations in the FKRP gene can cause muscle-eye-brain disease and Walker-Warburg syndrome. J Med Genet. 2004; 41:e61. [PubMed: 15121789]
8. van Reeuwijk J, et al. POMT2 mutations cause alpha-dystroglycan hypoglycosylation and Walker-Warburg syndrome. J Med Genet. 2005; 42:907–12. [PubMed: 15894594]
9. van Reeuwijk J, et al. Intragenic deletion in the LARGE gene causes Walker-Warburg syndrome. Hum Genet. 2007; 121:685–90. [PubMed: 17436019]
10. Silan F, et al. A new mutation of the fukutin gene in a non-Japanese patient. Ann Neurol. 2003; 53:392–6. [PubMed: 12601708]
11. Hara Y, et al. A dystroglycan mutation associated with limb-girdle muscular dystrophy. N Engl J Med. 2011; 364:939–46. [PubMed: 21388311]
12. Lefeber DJ, et al. Deficiency of Dol-P-Man synthase subunit DPM3 bridges the congenital disorders of glycosylation with the dystroglycanopathies. Am J Hum Genet. 2009; 85:76–86. [PubMed: 19576565]

13. Godfrey C, et al. Refining genotype phenotype correlations in muscular dystrophies with defective glycosylation of dystroglycan. Brain. 2007; 130:2725–35. [PubMed: 17878207]
14. Jimenez-Mallebrera C, et al. A comparative study of alpha-dystroglycan glycosylation in dystroglycanopathies suggests that the hypoglycosylation of alpha-dystroglycan does not consistently correlate with clinical severity. Brain Pathol. 2009; 19:596–611. [PubMed: 18691338]
15. Lin YY, et al. Zebrafish Fukutin family proteins link the unfolded protein response with dystroglycanopathies. Hum Mol Genet. 2011; 20:1763–75. [PubMed: 21317159]
16. Zhang Z, Zhang P, Hu H. LARGE expression augments the glycosylation of glycoproteins in addition to alpha-dystroglycan conferring laminin binding. PLoS One. 2011; 6:e19080. [PubMed: 21533062]
17. Bleckmann C, et al. O-glycosylation pattern of CD24 from mouse brain. Biol Chem. 2009; 390:627–45. [PubMed: 19284289]
18. Gilissen C, et al. Exome sequencing identifies WDR35 variants involved in Sensenbrenner syndrome. Am J Hum Genet. 2010; 87:418–23. [PubMed: 20817137]
19. Liu J, Mushegian A. Three monophyletic superfamilies account for the majority of the known glycosyltransferases. Protein Sci. 2003; 12:1418–31. [PubMed: 12824488]
20. Michele DE, et al. Post-translational disruption of dystroglycan-ligand interactions in congenital muscular dystrophies. Nature. 2002; 418:417–22. [PubMed: 12140558]
21. Snow CJ, et al. Time-lapse analysis and mathematical characterization elucidate novel mechanisms underlying muscle morphogenesis. PLoS Genet. 2008; 4:e1000219. [PubMed: 18833302]
22. Parsons MJ, et al. Zebrafish mutants identify an essential role for laminins in notochord formation. Development. 2002; 129:3137–46. [PubMed: 12070089]
23. Bassett DI, et al. Dystrophin is required for the formation of stable muscle attachments in the zebrafish embryo. Development. 2003; 130:5851–60. [PubMed: 14573513]
24. Straub V, Rafael JA, Chamberlain JS, Campbell KP. Animal models for muscular dystrophy show different patterns of sarcolemmal disruption. J Cell Biol. 1997; 139:375–85. [PubMed: 9334342]
25. Richard SB, et al. Kinetic analysis of Escherichia coli 2-C-methyl-D-erythritol-4-phosphate cytidyltransferase, wild type and mutants, reveals roles of active site amino acids. Biochemistry. 2004; 43:12189–97. [PubMed: 15379557]
26. Baur S, Marles-Wright J, Buckenmaier S, Lewis RJ, Vollmer W. Synthesis of CDP-activated ribitol for teichoic acid precursors in Streptococcus pneumoniae. J Bacteriol. 2009; 191:1200–10. [PubMed: 19074383]
27. MacLeod H, et al. A novel FKRP mutation in congenital muscular dystrophy disrupts the dystrophin glycoprotein complex. Neuromuscul Disord. 2007; 17:285–9. [PubMed: 17336067]
28. Wood AJ, et al. Abnormal vascular development in zebrafish models for fukutin and FKRP deficiency. Hum Mol Genet. 2011; 20:4879–90. [PubMed: 21926082]
29. McMullan DJ, et al. Molecular karyotyping of patients with unexplained mental retardation by SNP arrays: a multicenter study. Hum Mutat. 2009; 30:1082–92. [PubMed: 19388127]
30. Woods CG, et al. Quantification of homozygosity in consanguineous individuals with autosomal recessive disease. Am J Hum Genet. 2006; 78:889–96. [PubMed: 16642444]
31. Parsons MJ, Campos I, Hirst EM, Stemple DL. Removal of dystroglycan causes severe muscular dystrophy in zebrafish embryos. Development. 2002; 129:3505–12. [PubMed: 12091319]
32. Link V, Shevchenko A, Heisenberg CP. Proteomics of early zebrafish embryos. BMC Dev Biol. 2006; 6:1. [PubMed: 16412219]
33. Robu ME, et al. p53 activation by knockdown technologies. PLoS Genet. 2007; 3:e78. [PubMed: 17530925]
34. Ciruna B, Jenny A, Lee D, Mlodzik M, Schier AF. Planar cell polarity signalling couples cell division and morphogenesis during neurulation. Nature. 2006; 439:220–4. [PubMed: 16407953]
35. Hall TE, et al. The zebrafish candyfloss mutant implicates extracellular matrix adhesion failure in laminin alpha2-deficient congenital muscular dystrophy. Proc Natl Acad Sci U S A. 2007; 104:7092–7. [PubMed: 17438294]

36. Venselaar H, Te Beek TA, Kuipers RK, Hekkelman ML, Vriend G. Protein structure analysis of mutations causing inheritable diseases. An e-Science approach with life scientist friendly interfaces. BMC Bioinformatics. 2010; 11:548. [PubMed: 21059217]

37. Kemp LE, Bond CS, Hunter WN. Structure of a tetragonal crystal form of Escherichia coli 2-C-methyl-D-erythritol 4-phosphate cytidylyltransferase. Acta Crystallogr D Biol Crystallogr. 2003; 59:607–10. [PubMed: 12595740]

Europe PMC Funders Author Manuscripts

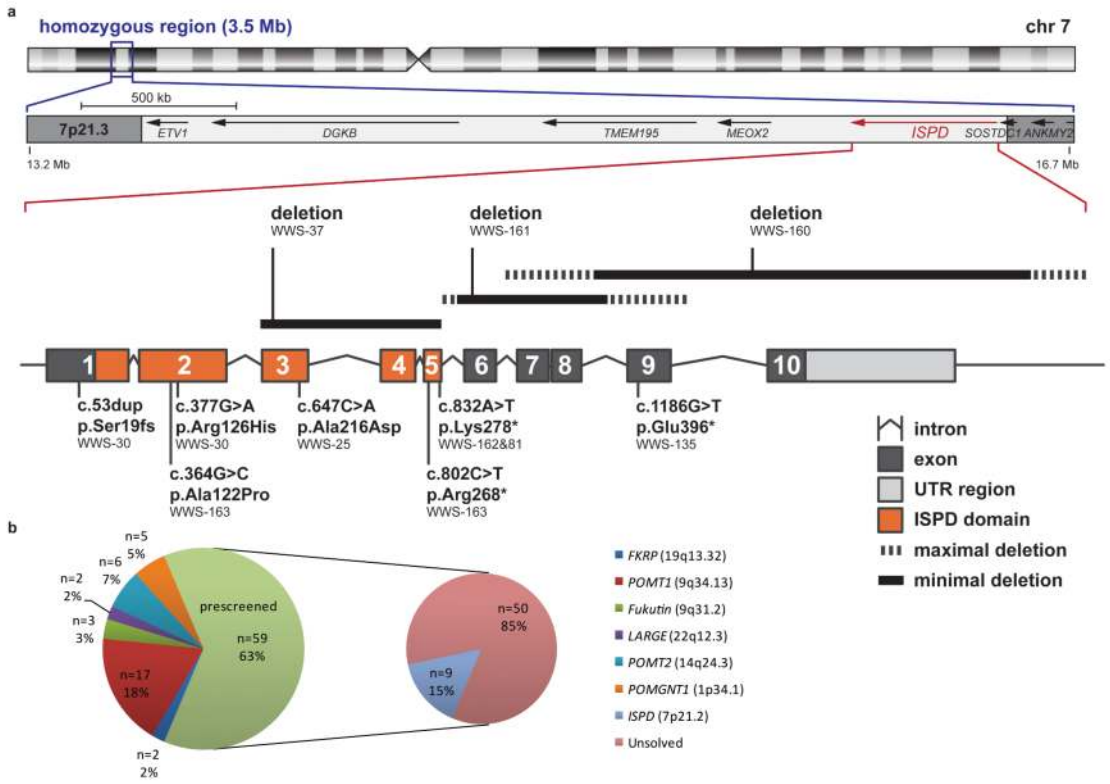

Figure 1.

Overview of genetic data in the patient cohort. (a) Schematic representation of the intragenic deletions, point mutations and homozygosity mapping data from WWS families with *ISPD* mutations. Ideogram of chromosome 7 showing the 3.5 Mb region of common homozygosity at band 7p21.3 flanked by SNPs rs194034 and rs818323 that was identified in family WWS-25. The position of three partially overlapping intragenic deletions in *ISPD* is indicated above the intron-exon structure of the gene. At the bottom the position of homozygous and compound heterozygous mutations is shown with respect to the ISPD protein domain structure. (b) Identified mutations in our total WWS/MEB cohort in number and percentage per gene. 94 families were available for research and prescreening revealed mutations in one of the six known genes in 35 families.

Europe PMC Funders Author Manuscripts

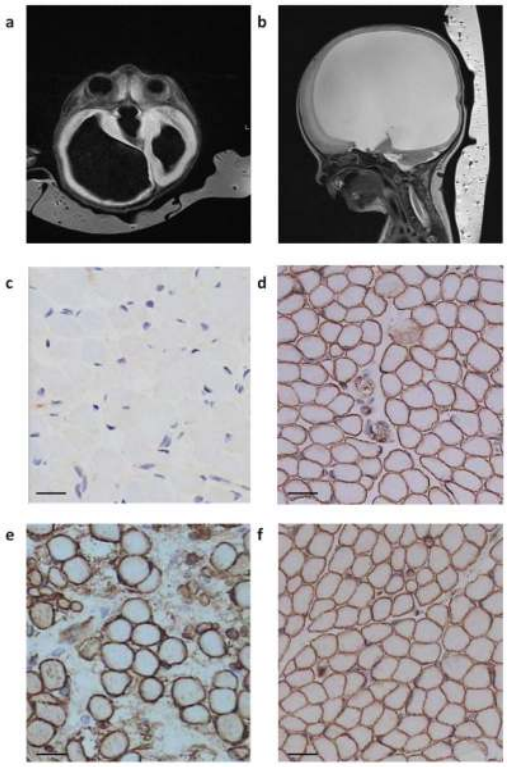

Figure 2.
MR images and muscle staining of patient WWS-160. (a) Axial T1 weighted and (b) parasagittal T2 cerebral MRIs showing hydrocephalus. (c) Muscle biopsy showed almost absent αDG glycosylation using IIH6 antibody in muscle in comparison to (d) IIH6 staining in a normal control muscle biopsy. (e) Spectrin staining in the patient was not visibly different from (f) normal control spectrin staining. Scale bars, 20 μm.

Europe PMC Funders Author Manuscripts

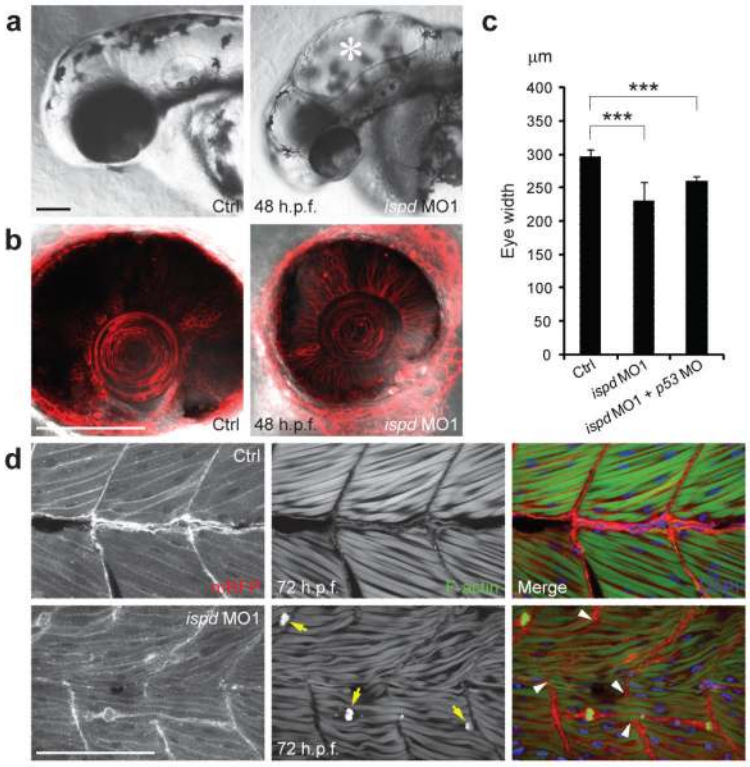

Figure 3.

Knockdown of zebrafish *ispd* recapitulates pathological defects of human WWS. (a) Compared with uninjected controls, zebrafish embryos injected with *ispd* MO1 (7 ng) showed characteristic hydrocephalus (asterisk) by 48 h.p.f. Scale bar, 100 µm. (b) Embryos injected with *ispd* MO1 (7 ng) showed microphthalmia by 48 h.p.f. in comparison to controls; cell membranes were visualized by membrane-localized red fluorescent protein (mRFP). Scale bar, 100 µm. (c) Eye width measurements in control (297.52±9.06 µm, n=25) and *ispd* MO1 (7 ng) injected embryos (230.8±28.35 µm, n=25; ***P= 4.68E-12). Co-injection of *p53* MO (6 ng) with *ispd* MO1 (6 ng) still resulted in reduced eye size (260.28 ± 6.86 µm, n=25; ***P= 1.39E-20), suggesting that this phenotype was not a consequence of MO off-target effects mediated by p53-induced cell death. Error bars indicate s.d. (d) Control embryos display intact muscle fibers that anchor to chevron-shaped MTJ. Embryos injected with *ispd* MO1 (7 ng) showed muscle fiber degeneration by 72 h.p.f. Retracting muscle fibers were revealed by condensed F-actin (arrows) and collapsed sarcolemma (visualized by mRFP). Abnormally elongated muscle fibers spanned disrupted MTJ (arrowheads) in zebrafish embryos lacking Ispd. DAPI indicates nuclei. Scale bar, 100 µm.

Europe PMC Funders Author Manuscripts

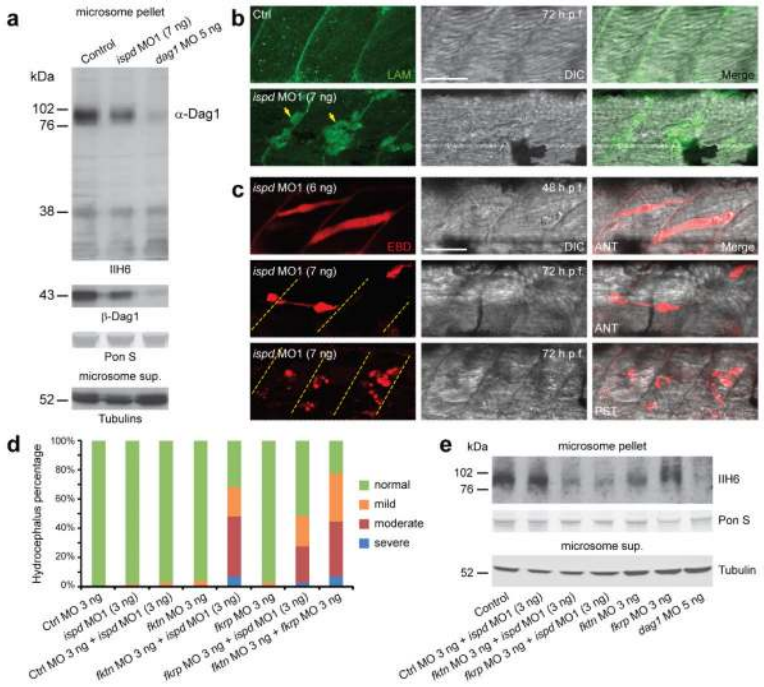

Figure 4.

Hypoglycosylation of αDG and disrupted sarcolemma integrity in *ispd* MO1-injected zebrafish embryos. (a) Western blot analysis of microsome pellets and supernatant from control, *ispd* MO1 (7 ng) and *dag1* MO (5 ng) injected embryos at 48 h.p.f. Compared with control embryos, *ispd* MO1-injected embryos showed a reduction of glycosylated αDG (IIH6; 76-102 kDa) with a slight decrease of ßDG, which is probably a secondary reduction due to protein instability caused by defective glycosylation of αDG as reported previously[27,28]. Both glycosylated αDG and ßDG were almost absent in *dag1* MO-injected embryos. Equal protein loading was demonstrated by Ponceau S (PonS) staining and unknown glycoproteins detected by IIH6 antibody in all three lanes (<38 kDa). Equivalent amounts of γ- and acetylated tubulins were detected in corresponding microsome supernatant. (b) Laminins remained localized at the MTJ in *ispd* MO1-injected embryos (7 ng). Positive fluorescent signal within degenerated muscle fibers (arrows) was probably due to disrupted sarcolemma integrity. Scale bar, 50 μm. (c) MTJ-anchored muscle fibers were infiltrated by EBD in *ispd* MO1-injected embryos before the onset of muscle degeneration. Dashed lines indicate MTJ. DIC, differential interference contrast microscopy; ANT, anterior myotome; PST, posterior myotome. Scale bar, 50 μm. (d) Injection of sub-effective doses of *ispd*, *fktn*, *fkrp* and control MO together or alone. Increase in the percentage of embryos with hydrocephalus suggests genetic interactions between *ispd*, *fktn* and *fkrp*. Each bar represents a combination of two independent experiments, scored blindly according to criteria exemplified in Supplementary Fig. 8a. n=94–139 embryos. (e) Western blotting with IIH6 antibody showed a reduction of glycosylated αDG in embryos co-injected with *ispd* MO1 and *fktn/fkrp* MO as compared to control MO and *ispd* MO1 co-injected embryos, and single *fktn* or *fkrp* MO-injected embryos. As a negative control, almost absent αDG glycosylation is shown for *dag1* MO injected embryos.

Europe PMC Funders Author Manuscripts

Europe PMC Funders Author Manuscripts

Table 1

Overview of *ISPD* mutations

Family	Diagnosis	Genomic position chr 7 (hg19)	Mutation	State	Exon(s) affected	Amino acid change	Segre-gation
WWS-25	WWS/MEB	g.16415754	c.647C>A	Homozygous	3	p.Ala216Asp	F, M
WWS-160	WWS	g.16078412-g.16279290	deletion[#]	Homozygous	9-10		F, M
WWS-161	WWS	g.16270332-g.16324185	deletion[#]	Homozygous	6-8		F, M
WWS-37	WWS		deletion[#]	Homozygous	3-5		NA
WWS-162	WWS	g.16341049	c.832A>T	Homozygous	5	p.Lys278*	F, M
WWS-81	MEB	g.16341049	c.832A>T	Homozygous	5	p.Lys278*	F, M
WWS-135	WWS	g.16255756	c.1186G>T	Homozygous	9	p.Glu396*	F, M
WWS-30	WWS	g.16460895	c.53dup	Heterozygous	1	p.Ser19fs	F
		g.16445843	c.377G>A	Heterozygous	2	p.Arg126His	M
WWS-163	MEB	g.16445856	c.364G>C	Heterozygous	2	p.Ala122Pro	M
		g.16341079	c.802C>T	Heterozygous	5	p.Arg268*	F

WWS, Walker–Warburg syndrome; MEB, Muscle Eye Brain disease; F, heterozygous in father; M, heterozygous in mother; NA, not available.

[#]The minimum deletion sizes are indicated. The genomic positions for WWS-160 and WWS-161 correspond to endpoints defined by SNPs that are homozygous deleted as determined by CNV analysis.